Preparation and Characterization of Cellulose/Ag Nanocomposites

Yongjian Xu,[1,2] Leigang Zuo,[1,2] Tao Lin,[1] Jiayong Wang,[1] Xiaopeng Yue[1]
[1]*College of Light Industry and Energy, Shaanxi University of Science and Technology, Shaanxi Province Key Lab of Paper Technology and Specialty Paper, Xi'an, 710021 China*

[2]*State Key Laboratory of Pulp and Paper Engineering, South China University of Technology, Guangzhou, 510640*

A simple, green, and efficient microwave-assisted heating method was developed to synthesize the cellulose/Ag nanocomposites by reducing silver nitrate in aqueous solution. The structure of nanocomposites was analyzed with X-ray diffraction and Fourier transform infrared, the results showed that nanosilver particles were synthesized successfully on the surface of cellulose and did not change the structure of cellulose obviously. The shape and average size of silver nanoparticles and its distribution on cellulose fiber surface were observed by scanning electron microscopy, and the results demonstrated that the silver nanoparticles had a good distribution on the surface of cellulose fiber and high dosage of polyvinyl pyrrolidone decreased the size of nanosilver particles. Atomic absorption spectroscopy was used to measure the silver content in the composites, it was found that the silver content was higher in composites obtained by microwave heating compared with oil bath heating. The effect of silver nanoparticles on the thermal stability of cellulose fiber was studied by thermogravimetric analysis and differential scanning calorimetry, and it revealed that the silver nanoparticles had no obvious influence on the thermal stability of cellulose. The excellent antimicrobial activity against both *Escherichia coli* (gram-negative bacteria) and *Staphylococcus aureus* (gram-positive bacteria) showed a potential application in medical and health care field. POLYM. COMPOS., 36:2220–2229, 2015. © **2014 Society of Plastics Engineers**

INTRODUCTION

As a kind of renewable natural polymer material, cellulose has the advantages of abundant source, low price, and pollution-free, and is used widely in our daily life. In recent years, nanocomposites have received comprehensively attention and have been widely studied due to their excellent properties [1–4]. As an important kind of nanocomposites, cellulose-based nanocomposites also attracted much attention. Until now, many kinds of cellulose-based nanocomposites have been studied, such as titanium dioxide/cellulose nanocomposites [5], hydroxyapatite/bacterial cellulose nanocomposites [6], CdS/regenerated cellulose nanocomposites [7], and $CaCO_3$/cellulose nanocomposites [8].

As a kind of cellulose-based nanocomposites, cellulose/Ag nanocomposites contain cellulose and silver nanoparticles. It is well known that silver ions and silver compounds have broad-spectrum antimicrobial activity, can wipe out nearly 650 types of bacteria [9], and have been used to control the growth and spread of bacteria in various applications, such as catheters, burn wounds, and dental work [10, 11]. Compared with silver ions and silver compounds, silver nanoparticles have more excellent antibacterial activity due to their larger specific surface area with decreasingly smaller silver particles [12, 13], the excellent antibacterial activity makes its application in medical and health care field possible. Generally, silver nanoparticles can be obtained directly from metallic silver [14], or be obtained by the reduction of silver ions in different ways, such as chemical reduction [15], light reduction [16], and electrochemical reduction [17]. Due to their simplicity, convenience and controllability, chemical reduction has become one of the most important methods to obtain silver nanoparticles. It would be able to endow cellulose with excellent antibacterial activity using cellulose as a template and embedding silver nanoparticles in. There have been some reports on the fabrication of the cellulose/Ag nanocomposites. For example, Maneerung et al. [18] obtained cellulose/Ag nanocomposites with

Correspondence to: L. Zuo; e-mail: zlgyjpa@outlook.com
Contract grant sponsor: National Natural Science Foundation of China; contract grant number: 31170559; contract grant sponsor: Academic Leaders Group Fund; contract grant number: 2013XSD25; contract grant sponsor: Open fund of National Key Laboratory of Pulp and Paper Engineering and South China University of Technology, contract grant number: 201465.
DOI 10.1002/pc.23134
Published online in Wiley Online Library (wileyonlinelibrary.com).

excellent antibacterial activity by immersing bacterial cellulose in the $AgNO_3$ solution and silver ions were reduced with sodium borohydride subsequently. Barud et al. [19] immersed bacterial cellulose in the mixed solution of $AgNO_3$ and triethanolamine for 12 h, and then, cellulose/Ag nanocomposites were successfully obtained by refluxing in ethanol solution subsequently after washing several times. Recently, Montazer et al. [20] obtained cellulose/Ag nanocomposites by treating cotton fabric with the solution of $[Ag(NH_3)]^+$ and the temperature of the solution was increased to the boil at a rate of 4°C/min for 30min.

In recent years, microwave was used in the synthesis of nanoparticles and nanocomposites due to its unique effects such as uniform heating, high reaction rate, reaction time saving, and energy saving [21, 22], such as carbon-supported PtSn nanoparticles, Co-ferrite nanoparticles, silver nanoparticles, Ag/ZnO nanocomposites, 2-hydroxyethyl methacrylate–chitosan/carbon nanotubes nanocomposites [23–27]. Microwave also can be used in the synthesis of cellulose/Ag nanocomposites. For example, Li et al. [28] has successfully obtained the cellulose/Ag nanocomposites by immersing microcrystalline cellulose in the ethylene glycol solution of silver nitrate with microwave-assisted heating subsequently. But these methods to obtain cellulose/Ag nanocomposites were still complex, costly and some harmful chemicals were used in the process, which was not good to reduce the cost of production and may have potential adverse effect in the application of the medical and health care field. Therefore, it is necessary to synthesize the cellulose/Ag nanoparticles in a simple, cheap, and green route.

As a mild and cheap reducer, glucose can be used for the reduction of silver ions in the synthesis of silver nanoparticles [29, 30]. Polyvinyl pyrrolidone (PVP) is often used as protective agent to prevent silver nanoparticles from agglomerating in the production process of silver nanoparticles [31, 32]. As a normal material, water is simpler and cheaper than organic solvents, ionic liquids, and other solution. In this article, we chose glucose as reducer and PVP as protective agent to obtain the cellulose/Ag nanocomposites in aqueous solution with microwave-assisted heating. The amount of PVP and $AgNO_3$ on the effect of the size and shape of silver nanoparticles, the content of nanosilver particles in composites and silver ions' utilization rate were also investigated. Moreover, the antibacterial activity of cellulose/Ag nanocomposites against *Escherichia coli* (gram-negative) and *Staphylococcus aureus* (gram-positive) was investigated by the inhibition zone and sterilization rate.

EXPERIMENTAL

Materials

Cellulose fiber, fully bleached chemical pulp derived from softwood, provided by Xiangtai Cellulose Corporation (Hubei Province, China). Silver nitrate (≥99.7%,) purchased from Shanghai Chemicals Corporation. Glucose (AR), provided by Fine Chemical Co., Tianjin North. PVP was delivered by BASF (Germany). All chemicals were used without further purification.

Preparation of Cellulose/Ag Nanocomposites

Cellulose fiber was dispersed into individual fiber before used. To obtain cellulose/Ag nanocomposites, 0.1 g glucose and 0.1 g PVP were added into beaker with a certain amount of distilled water under magnetic stirring. After glucose and PVP dissolved, 1.0 g cellulose fiber was added and made it disperse homogeneously in the system with magnetic stirring. Then the different volumes of 0.01 M $AgNO_3$ solution were added drop by drop and kept the total volume of solution 150 mL. After 15 min of stirring dispersion, the beaker was put into microwave and heated at 560 W for 10 min and then air cooled to room temperature naturally. Finally the product was washed three times by water and dried at 105°C.

Characterization

The morphology of cellulose/Ag nanocomposites was observed by a TM-1000 scanning electron microscopy (SEM, HITACHI, Japan). Histograms of size distribution were calculated from the SEM images by measuring the diameters of at least 100 particles. The structure of the nanocomposites was identified by Fourier transform infrared (FTIR) spectroscopy using a NEXUS 670 FTIR (Thermo Fisher Nicolet, USA) instrument with KBr sample disks. X-ray diffraction (XRD) patterns of cellulose/Ag nanocomposites were recorded with D/max 2200 X-ray diffractometer (RIGAKU company, Japan) using Cu Kα radiation ($\lambda = 1.5406$ Å) operating at 45 kV. The patterns were recorded in the range of $2\theta = 5°–85°$. Thermogravimetric (TG) analysis and differential scanning calorimetry (DSC) were performed on a SDT Q600 apparatus (TA Instruments, USA) at a heating rate of 10°C/min from 35°C to 800°C under nitrogen atmosphere. The silver content of composites was measured by atomic absorption spectroscopy (AAS, HITACHI, Japan), and the sample was dissolved by concentrated nitric acid with heating before measuring.

Antibacterial Properties

The antibacterial activity of cellulose/Ag nanocomposites against *E. coli* as the representative of gram-negative bacteria and *S. aureus* as the representative of gram-positive bacteria were evaluated by agar diffusion method. The medium was prepared as follows: 0.5 g beef extract, 0.5 g sodium chloride, 1.0 g peptone, and 1.5 g agar were added into 100 mL distilled water and autoclaved at 121°C for 15 min. Afterward, 20 mL medium was poured into sterilized Petri dish. After the medium

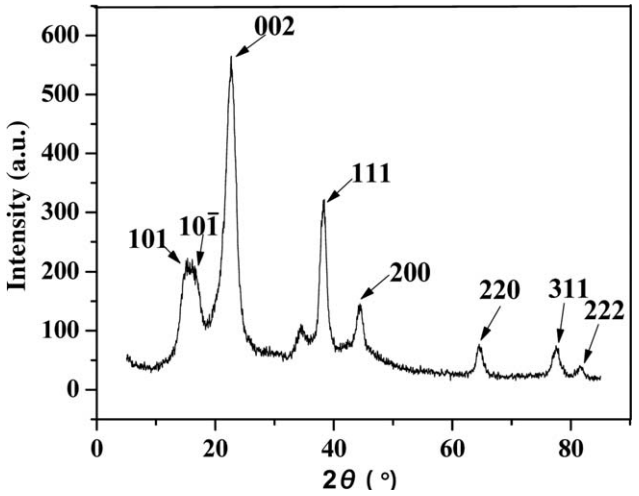

FIG. 1. XRD pattern of the cellulose/Ag nanocomposites.

solidified, 50 μL bacterial suspensions were uniformly smeared over the dish. Then, circular pieces of 14-mm diameter of the cellulose control and the nanocomposites samples were gently placed on Petri dishes. Then the diameter of the inhibition zone was measured after incubated for 24 h at 37°C. The sterilization rate of composites was measured as follows: 0.1 g composites were added to the 100 mL of fresh *E. coli* or *S. aureus* culture at a concentration of 10^6 colonies forming units per mL (cfu/mL), and then incubated in shaking incubator at 37°C for different time. After that, 50 μL bacterial suspensions were drawn from each of Petri dishes. The same procedure was performed on pure cellulose. The sterilization rate in bacterial count was calculated by the formula [33]:

$$\frac{(\text{Viable count at } 0\,\text{min} - \text{viable count at different time})}{\text{Viable count at } 0\text{min}} \times 100\%$$

RESULTS AND DISCUSSION

Crystal Structure of the Nanocomposites

Figure 1 is the XRD pattern of cellulose/Ag nanocomposites obtained by heating the solution of 1.0 g cellulose fiber, 0.1 g glucose, 0.1 g PVP, and 20 mL 0.01 M $AgNO_3$ solution for 10 min with microwave. In Fig. 1, the typical diffraction peaks assigned to cellulose and face-centered cubic silver nanoparticles were observed clearly. The diffraction peaks at around $2\theta = 15.2°$, 16.8°, and 22.8° were attributable to the101, 10$\bar{1}$, and 002 planes of cellulose I, respectively. And peaks at around $2\theta = 38.4°$, 44.2°, 64.4°, 77.3°, and 81.5° were assigned to the well-crystallized silver nanoparticles with face-centered cubic structure (JCPDS 04–0783). No other peaks from impurities were observed. It indicated that silver nanoparticles had been successfully reduced on the cellulose matrix under microwave-assisted heating.

Morphology of Nanocomposites

Figure 2 shows the morphology of cellulose/Ag nanocomposites prepared at the aqueous solution of 1.0 g cellulose, 0.1 g PVP, 0.1 g glucose, and different volume of $AgNO_3$ solution by microwave heating. Figure 3 is the size distribution of silver nanoparticles. In Fig. 2, it can be seen that the silver nanoparticles dispersed on the cellulose substrate homogeneously. When the volume of $AgNO_3$ solution was 5 mL, there were a few silver nanoparticles homogeneously dispersed in the cellulose matrix. Moreover, the silver nanoparticles were cubic and had a narrow size distribution with an average particle size of about 50 nm. The emergence of cubic silver nanoparticles could be explained that the selective adsorption of PVP on the 100 plane of silver nanoparticles would lead to the growth rate in other lattice planes was faster than the 100 plane and resulted in the formation of cubic silver nanoparticles eventually [34, 35]. When 10 mL $AgNO_3$ solution was added, many silver nanoparticles emerged on the surface of cellulose with a uniform distribution and both large and small particles were observed. At the same time, both the cubic and spherical silver nanoparticles appeared on the surface of cellulose fiber. The size distribution was wide compared with (a), and most of nanosilver was found to be about 40 nm. When the volume of $AgNO_3$ solution was increased to 20 mL, it can be seen

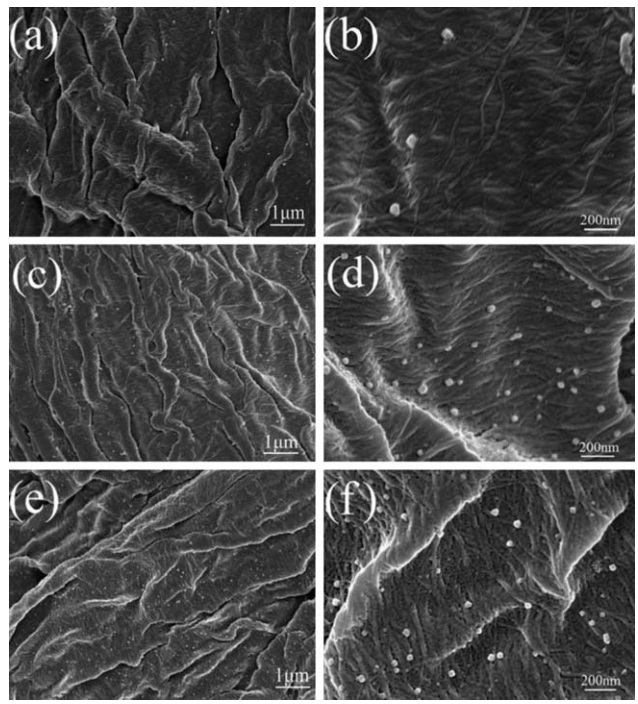

FIG. 2. SEM micrographs of cellulose/Ag nanocomposites prepared at the different amount of silver nitrate solution: (a and b) 5 mL; (c and d) 10 mL; and (e and f) 20 mL.

DOI 10.1002/pc

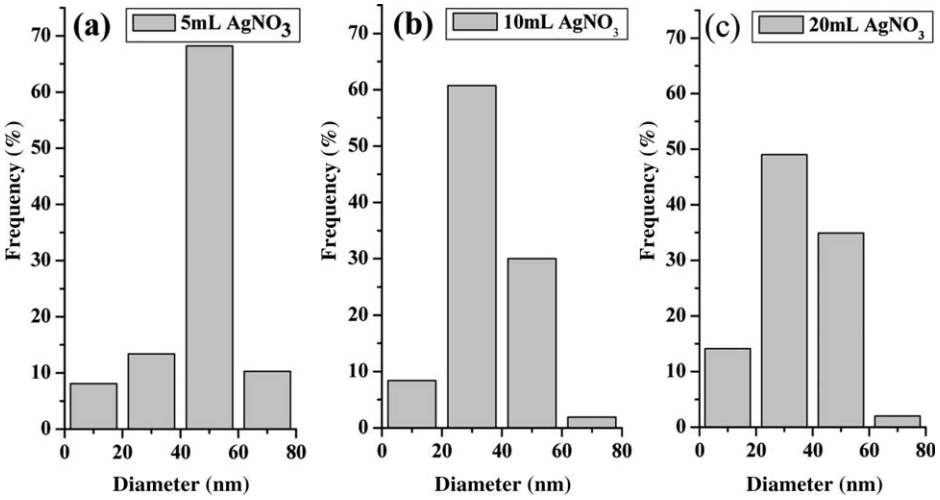

FIG. 3. The size distribution of silver nanoparticles.

that there were more silver nanoparticles dispersed on the surface of cellulose without agglomeration and the size distribution of nanoparticles was similar to (b).

There were no agglomeration occurred and nanosilver particles transformed from cube to spherical gradually with the increasing amount of $AgNO_3$, which can be explained that cellulose is a kind of macromolecular polysaccharide consisting of D-glucose with β-1,4 glycosidic bonds, and there are three OH groups in each glucose unit. Quantities of electron-rich oxygen atoms in the OH group and ether group of cellulose can interact with transition metal cations, therefore, the silver ions can be absorbed on the surface of cellulose macromolecules by electrostatic interaction, resulted silver ions were difficult to move freely. So, the particles were hard to agglomerate and form large particles during the reduction process. Besides, PVP was not enough to control the shape of nanosilver particles with increasing amount of $AgNO_3$. As a result, the number of spherical particles was more than cubic particles.

The Effect of PVP on the Morphology of Nanocomposites

The influence of the amount of PVP on the size and shape of silver nanoparticles was also investigated, as shown in Figs. 4 and 5. The SEM graphs of cellulose/Ag

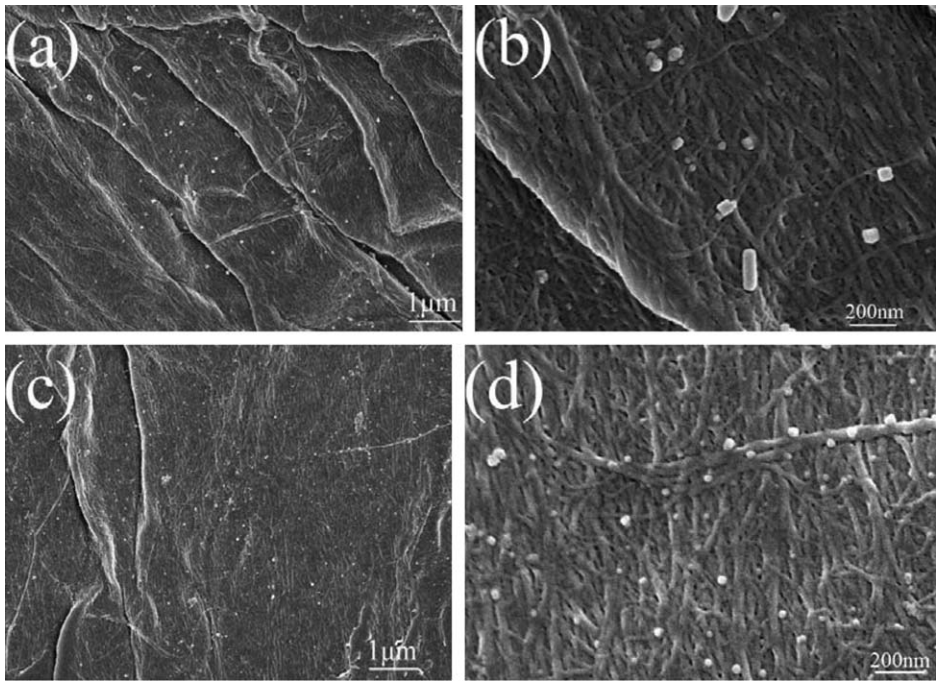

FIG. 4. SEM micrographs of cellulose/Ag nanocomposites prepared with 1.0 g cellulose, 0.1 g glucose, 20 mL 0.01 M $AgNO_3$ solution, and different amount of PVP: 0.4 g PVP (a and b), 0.8 g PVP (c and d).

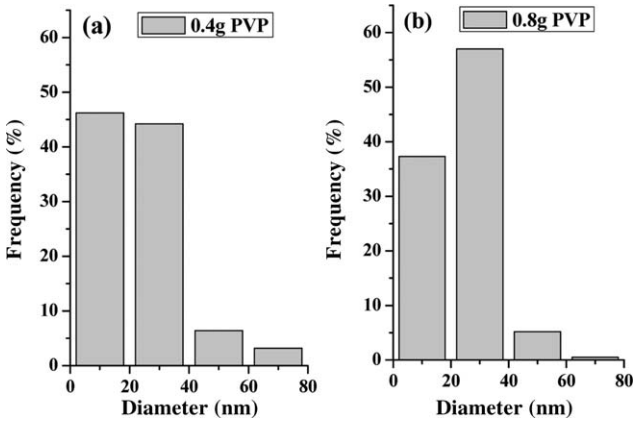

FIG. 5. The size distribution of silver nanoparticles.

nanocomposites were obtained by heating the aqueous solution of 1.0 g cellulose fiber, 0.1 g glucose, 20 mL 0.01 M $AgNO_3$ solution, and different amount of PVP with microwave. When 0.4 g PVP was added, it had a same molar ratio between PVP and $AgNO_3$ compared with (a) and (b) in Fig. 2, some cubic silver nanoparticles with large size can be observed obviously, but most of the nanosilver particles had a size smaller than 40 nm. When 0.8 g PVP was added, large number of spherical silver nanoparticles with smaller size of about 20 nm had a uniform distribution on the surface of cellulose fiber. With increasing amount of PVP, more and more small particles were formed. It was concluded that a large number of small silver nuclei were generated and covered by PVP at the beginning of reductive action. This result indicated that high dosage of PVP was conducive to the formation of spherical silver nanoparticles with smaller size.

Structure Analysis of Nanocomposites

The FTIR analysis was used to observe the structural changes of nanocomposites. Figure 6a is the FTIR spectra of cellulose without silver nanoparticles, (b), (c) and (d) are the FTIR spectra of cellulose/Ag nanocomposites obtained with 5, 10, and 20mL 0.01 M $AgNO_3$ solution added with microwave-assistant heating, respectively. For cellulose/Ag nanocomposites, the large absorption band centered at around 3,424 cm^{-1} is attributed to the stretching vibration of hydroxyl group and hydrogen bond; the band at 2,901 cm^{-1} is assigned to the asymmetrical stretching vibration of C—H in pyranoid ring [36]. It can also be noted that the peaks at 1,431 cm^{-1} corresponded to the symmetric bending of CH_2; the band at 1,373 cm^{-1} is assigned to the OH bending vibration [37]; the band at 1,319 cm^{-1} is assigned to the C—C and C—O skeletal vibration [38]; the band at 1,165 cm^{-1} belongs to the C—O antisymmetric bridge stretching; and 1,059 cm^{-1} is attributed to C—O—C pyranose ring skeletal vibration [39]. As shown in Fig. 6, the FTIR spectrums of nanocomposites were similar to the IR spectrum of pure cellulose; it indicated that there were no obvious changes happened in the structure of cellulose.

TG/DSC Analysis of Nanocomposites

The thermal stability of cellulose/Ag nanocomposites was investigated by TG and DSC, as shown in Fig. 7. From TG curves, there were two main stages of weight loss. For pure cellulose fiber: a small weight loss about 7.8% happened when the temperature increased from 35°C to 100°C, which was caused by the loss of hydrated and coordinated water molecules; when the temperature increased to about 300°C, a repaid decrease of weight began to happen due to the thermal degradation and decomposition of cellulose fiber, and there was a low solid residue (about 5.5%) left when the temperature increased to 800°C. For the nanocomposites, it had a familiar TG cure compared to pure cellulose. There was 8.5% mass loss when the temperature increased to 100°C and the residual mass (22.7%) obtained for temperature at 800°C was related to silver particles.

In the DSC cures, the pure cellulose fiber showed two endothermic peaks at the temperature 349°C and 370°C, which were the thermal degradation and decomposition of cellulose fiber, respectively. And they were so close, this maybe was the reason why it was difficult to distinguish them on the TG curve. Under 400°C, DSC cure of nanocomposites was similar to DSC curve of pure cellulose fiber, but after embedded silver nanoparticles in cellulose, the thermal degradation peak of cellulose moved from 349°C to 337°C, indicating that the thermal stability of nanocomposites had slight decrease compared with pure cellulose fiber. Besides, the behavior of curve (b) was different with respect to curve (a) when the temperature was

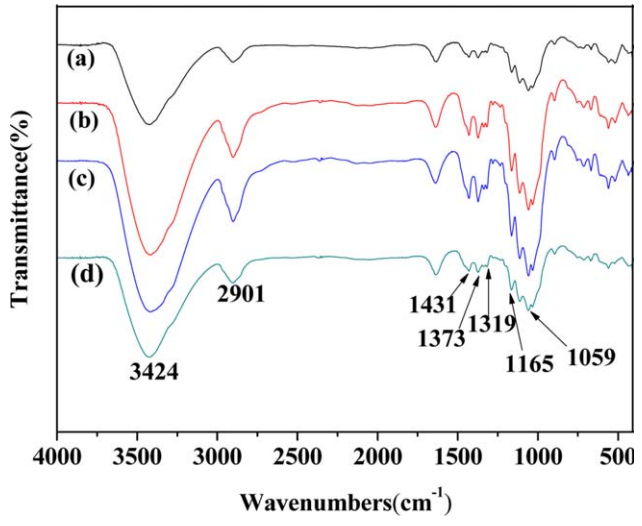

FIG. 6. FTIR spectra of cellulose/Ag nanocomposites prepared with 1.0 g cellulose, 0.1 g glucose, 0.1 g PVP, and different amount of 0.01 M $AgNO_3$ solution: 0 mL (a), 5 mL (b), 10 mL (c), and 20 mL (d). [Color figure can be viewed in the online issue, which is available at wileyonlinelibrary.com.]

DOI 10.1002/pc

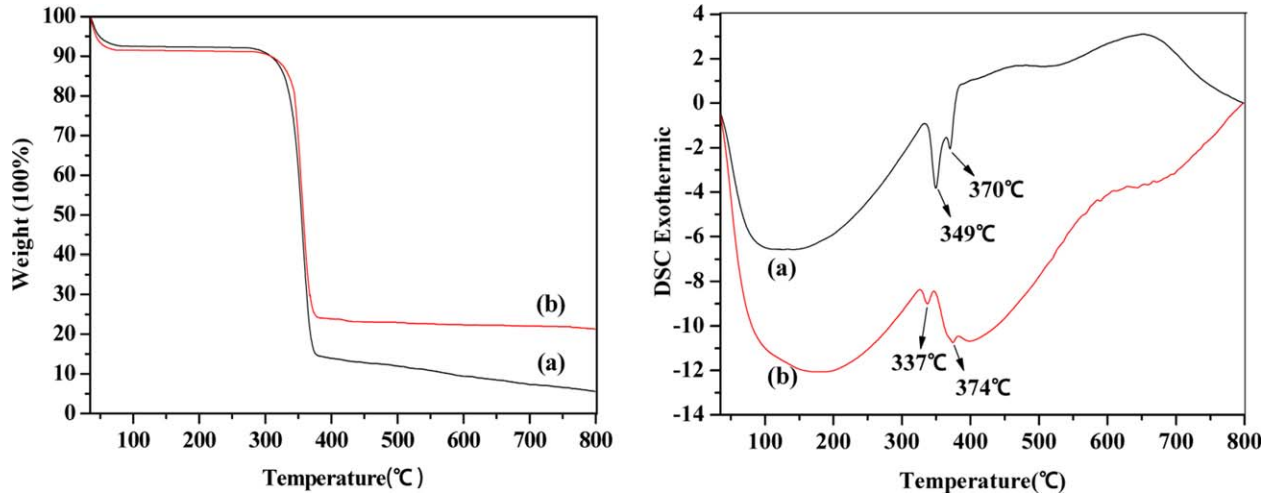

FIG. 7. TG and DSC curves of the cellulose/Ag nanocomposites: (a) is the control; b is the sample which 20 mL 0.01 M $AgNO_3$ solution was added. [Color figure can be viewed in the online issue, which is available at wileyonlinelibrary.com.]

above 400°C. When the temperature increased to 400°C, the DSC value of curve (a) was above zero, but the DSC value of curve (b) was under zero. From 400°C to 600°C, DSC value of curve (a) was stable but after that it started increasing with temperature increasing further. It might relate to the cracking of some functional groups in cellulose residue. When the temperature was above 400°C, the residual would produce some kinds of gases in the charring procession of cellulose [40], and Ball et al. [41] pointed out that the char formation of cellulose was a low activation energy exothermal process and volatilization was a high activation energy endothermal process. The DSC value of curve (b) was still under zero with the temperature was between 400°C to 800°C, it may be due to that the silver particles may played a positive role for the release of gas in the charring process of cellulose. These results indicated that the thermal stability of cellulose/Ag nanoparticles had no obvious decrease compared with pure cellulose fiber, but the silver particles can encourage the release of gas in the charring process of cellulose.

Silver Content Variation of Cellulose/Ag Nanocomposites

The silver content variation of composites measured by AAS and the results are shown in Figs. 8 and 9. Figure 8 shows the silver content variation of nanocomposites prepared at different conditions: curve (a) was obtained by heating the aqueous solution of 1.0 g cellulose, 0.1 g PVP, 0.1 g glucose, and different amount of $AgNO_3$ solution with microwave; curve (b) was obtained without glucose compared with (a); curve (c) was obtained by replacing microwave heating with oil bath

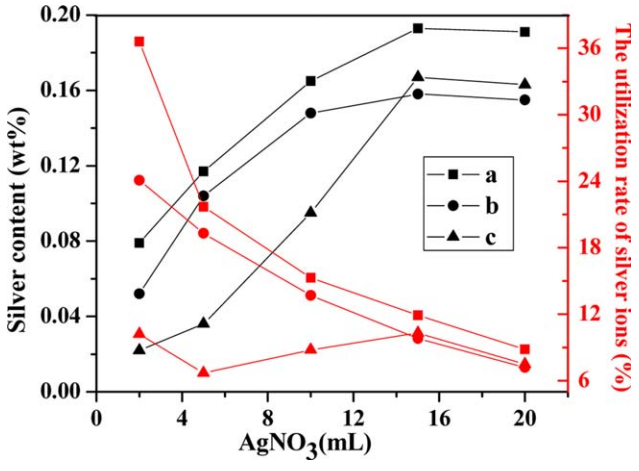

FIG. 8. The variation of silver content and silver ions' utilization rate in nanocomposites prepared with different methods: MW (a and b) and oil bath heating (c). [Color figure can be viewed in the online issue, which is available at wileyonlinelibrary.com.]

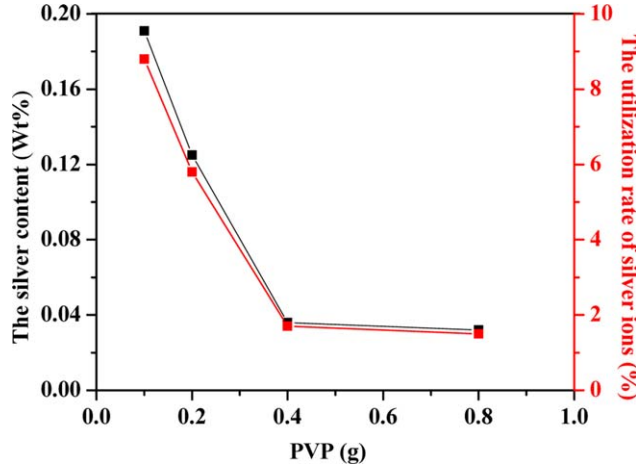

FIG. 9. The silver variation and silver ions' utilization rate in composites obtained with 1.0 g cellulose, 0.1 g glucose, 20 mL 0.01 M $AgNO_3$ solution, and different amount of PVP. [Color figure can be viewed in the online issue, which is available at wileyonlinelibrary.com.]

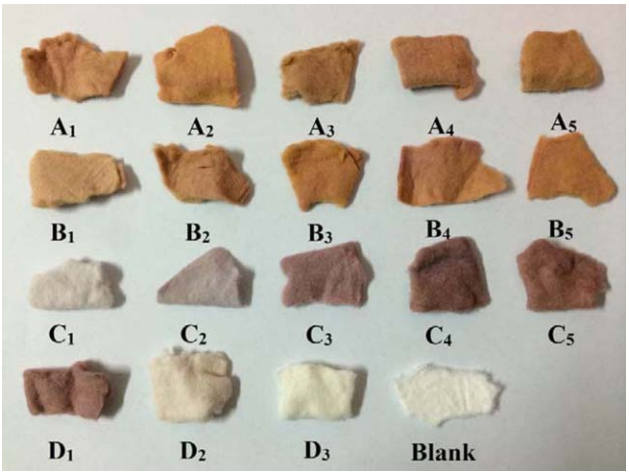

FIG. 10. The color variation of cellulose/Ag nanocomposites prepared at different ways: microwave heating (A), microwave heating without glucose (B), oil bath heating (C), microwave heating with different amount of PVP. [Color figure can be viewed in the online issue, which is available at wileyonlinelibrary.com.]

heating at 130°C for 40 min compared with curve (a). Figure 9 is the effect of the dosage of PVP on the silver content of composites prepared by heating the aqueous solution of 1.0 g cellulose, 0.1 g glucose, 20 mL 0.01 M $AgNO_3$ solution, and different amount of PVP with microwave.

Figure 8 shows that the silver content increased with the increasing amount of $AgNO_3$ solution. Compared curve (a) with curve (b), curve (a) had higher silver content. Thought there was no glucose as reducer in curve (b), there was still similar silver content. It may be that the hemiacetal hydroxyl group in cellulose is reductive, which led to part of silver ions was reduced to nanosilver particles. Besides, PVP was also used as reducer in some reports, maybe the generation of nanosilver particles partly owed to the reducibility of PVP [42–44]. In Fig. 8, we can see that the silver content of nanocomposites prepared by oil bath heating [curve (c)] was lower than microwave heating [curve (a) and (b)], showing that microwave heating can improve the silver content of composites compared with oil bath heating. Furthermore, the utilization rate of silver was also investigated. In Fig. 8, the utilization rate of silver ions was decreased with the increasing of $AgNO_3$ amount [curve (a)–(c)], indicating high $AgNO_3$ amount was not conducive to improving the utilization rate of silver ions.

In Fig. 9, both the silver content and utilization rate of silver ions decreased with the increasing amount of PVP. As a protective agent, PVP can form a complex compound with silver ion and prevent the silver particles from aggregation by covering on the surface of the silver particles [45]. The increasing amount of PVP would lead to more formation of PVP-Ag^+ and more silver particles covered by PVP at the beginning of reductive action. Besides, the force between PVP and Ag^+ may be stronger than the electrostatic interaction between cellulose and Ag^+. Therefore, less silver particles formed on the surface of cellulose. This may explain why the silver content decreased with the increasing amount of PVP.

The Color Variation of Cellulose/Ag Nanocomposites

The color variation of cellulose/Ag nanocomposites obtained with different ways is shown as Fig. 10. The cellulose/Ag nanocomposites in Group A was obtained by heating the aqueous solution of 1.0 g cellulose, 0.1 g glucose, 0.1 g PVP, and different amount of 0.01 M $AgNO_3$ solution (A_1 2, A_2 5, A_3 10, A_4 15, and A_5 20 mL) with microwave. Group B was obtained without glucose compared with Group A. Group C was obtained by replacing microwave heating with oil bath heating at 130°C for 40 min compared with Group A. Group D changed the amount of PVP into 0.2 g (D_1), 0.4 g (D_2), and 0.8 g (D_3) compared with Sample A_5.

In Group A, we can see that the composites were yellow, and the color deepened slightly with the increasing amount of $AgNO_3$ solution. Compared with Group A, Group B had similar color and the color was also darker with the increasing amount of $AgNO_3$ solution. But, when changed microwave heating to oil bath heating, the color of composites changed greatly. When the amount of $AgNO_3$ solution was added from 2 mL increased to 20 mL (C_1–C_5), the color of composite changed from white to brown. In He et al.'s [46] report, the color of solution containing nanosilver will darken and change from yellow to brown with larger size of silver nanoparticles. This indicated that the size of nanosilver particles of composites obtained by oil bath heating was larger compared with microwave heating. In Group D, with increasing amount of PVP (D_1–D_3), the color of composites changed significantly from deep color to white. Cellulose itself (black) is white, and the composites have lower silver content and smaller silver particles with increasing amount of PVP, perhaps these were the reason that made the color of composites closer to the color of cellulose itself.

Antibacterial Activity

In Fig. 11, the pure cellulose fiber was used as control (S_0), and S_1, S_2, S_3, S_4, and S_5 corresponded to the nanocomposites obtained by adding 2, 5, 10, 15, and 20 mL 0.01 M $AgNO_3$ solution, respectively. For sample (d) and (d′), S_1, S_2, and S_3 corresponded to the nanocomposites achieved by adding 0.2, 0.4, and 0.8 g of PVP, respectively. Tables 1 and 2 were the growth inhibition rates corresponded to the Fig. 11.

The antibacterial activity of cellulose/Ag nanocomposites is very important for their application in biomedical fields. As we all know, silver nanoparticles have very excellent antimicrobial effect, but the antibacterial mechanism is still not fully understood. Some studies demonstrated that the surface of silver nanoparticles can generate free radical and induce the

 DOI 10.1002/pc

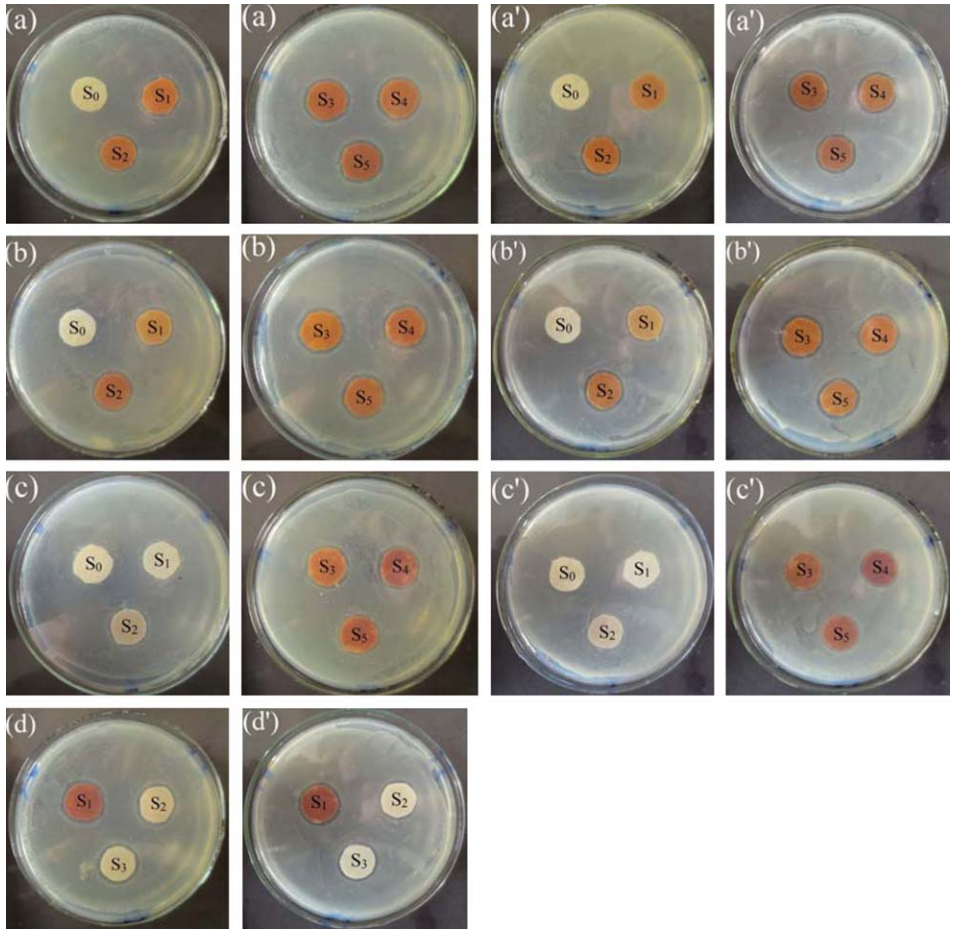

FIG. 11. Antibacterial activity of the cellulose/Ag nanocomposites: *E. coli* (a, b, c and d) and *S. aureus* (a′, b′, c′, and d′). [Color figure can be viewed in the online issue, which is available at wileyonlinelibrary.com.]

membrane damage subsequently [47]. Besides, the oxygen can easily oxidize silver nanoparticles to generate partially oxidized nano-Ag with chemisorbed Ag^+ that would lead to the destruction of the cell membrane, which could contribute the antibacterial activity to silver nanoparticles [48–51].

The antimicrobial activity of cellulose/Ag nanocomposites against *E. coli* and *S. aureus* was measured and the test results were shown in Fig. 11 and Tables 1 and 2. In Fig. 11, there were no inhibition zones exhibited around the pure cellulose fiber (S_0), indicating that the cellulose fiber alone did not have any antibacterial activity. When

TABLE 1. Sterilization rate of cellulose/Ag nanocomposites against *E. coli* and *S. aureus*.

			E. coli					*S. aureus*				
		$AgNO_3$/mL	2	5	10	15	20	2	5	10	15	20
Heating methods		Time/min										
MW	A	5	63.5	88.4	90.2	92.5	94.8	54.5	78.7	89.5	90.8	91.7
		10	90.3	94.6	95.2	96.1	98.4	84.5	89.6	93.1	94.3	96.4
		30	96.4	99.9	99.6	99.8	99.9	90.7	94.6	99.8	99.9	99.8
		60	99.7	99.9	99.9	99.9	99.9	99.7	99.9	99.8	99.8	99.9
	B	10	90.7	93.9	94.8	95.7	99.8	82.3	87.6	92.5	94.5	97.7
Oil bath	C	10	76.1	80.5	86.7	90.2	93.6	72.5	75.6	81.3	88.4	92.7

The composites in Group A were obtained by heating the aqueous solution of 1.0 g cellulose, 0.1 g glucose, 0.1 PVP, and different amount of 0.01 M $AgNO_3$ with microwave. Their sterilization rate was tested by adding 0.1 g composites into 100 mL of fresh *E. coli* or *S. aureus* culture at a concentration of 10^6 colonies forming units per mL (cfu/mL), and then incubated in shaking incubator at 37°C for different time.

The composites in Group B without glucose compared with Group A.

Group C was obtained by replacing microwave heating with oil bath heating at 130°C for 40 min compared with Group A.

TABLE 2. The effect of PVP amount on sterilization rate of cellulose/Ag nanocomposites.

	E. coli			*S. aureus*		
PVP/g	0.2	0.4	0.8	0.2	0.4	0.8
D (10 min)	97.7	99.8	98.6	98.5	99.9	99.9

Group D was obtained by heating the aqueous solution of 1.0 g cellulose, 0.1 g glucose, 20 mL 0.01 M $AgNO_3$, and different amount of PVP.

2 mL 0.01 M $AgNO_3$ solution was added, we can see that inhibition zones exhibited around S_1 in (a), (b), and (b′), and no inhibition zone exhibited around S_1 in (c) and (c′). With the increasing amount of $AgNO_3$ solution, the inhibition zones were growing. When more than 10 mL $AgNO_3$ solution was added, the inhibition zones have no obvious changed. This may be due to the silver content that did not increase much with $AgNO_3$ solution over 10 mL. Compared with the inhibition zones of composites obtained by microwave heating and oil bath heating, the former inhibition zones were bigger and clearer than the latter, indicating that the antibacterial activities of the composites obtained by microwave heating was better than oil bath heating. When 20 mL $AgNO_3$ solution was added, changing the dosage of PVP [(d) and (d′)], we can see that the inhibition zones did not change much in spite of the silver content reduced much. This indicated that the antibacterial activity was more excellent with decreasing nanosilver particles size even though the silver content reduced.

Tables 1 and 2 were the sterilization rate of composites. The sterilization rates of composites (A) against *E. coli* and *S. aureus* increased with the increasing amount of $AgNO_3$ solution and prolonged contact time. When the contact time was 5 min, more than half of the bacteria including *E. coli* and *S. aureus* were killed. In particular, above 90% of the bacteria were killed when more than 10 mL $AgNO_3$ solution was added. When the contact time was 60 min, we can see that more than 99% of the bacteria were killed in all samples. At the same time, the composites (B) obtained by microwave heating without glucose, it also had excellent antibacterial activity compared with A at the same contact time. Compared with composites (A) and (B), the composites (C) obtained by oil bath heating had low sterilization rate against both *E. coli* and *S. aureus*. In Table 2, increasing the dosage of PVP, we can see that the composites (D) had sterilization rate above 97% against both *E. coli* and *S. aureus* and were higher than composites (A). These results indicated that the antibacterial activity of composites was very excellent and it can kill 99% bacteria in a short time.

CONCLUSION

A simple, efficient, and green microwave-assisted route was successful developed for the synthesis of cellulose/Ag nanocomposites. XRD pattern revealed that the silver nanoparticles had the faced-centered cubic structure. The FTIR spectroscopy demonstrated that in the process of the synthesis of cellulose/Ag nanocomposites there were no significant structural changes happened in the cellulose fiber. The TG and DSC curves indicated that the thermal stability of nanocomposites has no obvious decrease compared with pure cellulose fiber, but the silver particles would accelerate the release of gas in the charring process of cellulose when the temperature was above 400°C. SEM showed that the amount of silver nanoparticles which was well-distributed on the surface of cellulose fiber increased and the utilization rate of silver ions decreased with increasing dosage of $AgNO_3$. High amount of PVP was conducive to the spherical nanosilver particles with smaller size, but it would decrease the silver content of composites. Compared with microwave heating, the composites obtained by oil bath heating had lower silver content, larger size, and darker color. The antibacterial test results of nanocomposites demonstrated it had a strong antimicrobial activity against both *E. coli* (gram-negative bacteria) and *S. aureus* (gram-positive bacteria), and most of bacteria can be killed in a short time. This demonstrates it has a potential application in the medical and health care field.

REFERENCES

1. M. Chi, J.S. Wu, and J.X. Li, *Polymer*, **43**, 2981 (2002).
2. M. Alexandre and P. Dubois. *Mater. Sci. Eng. R*, **28**, 1 (2000).
3. W. Caseri, *Macromol. Rapid Commun*., **21**, 705 (2000).
4. M. Haghayegh and G. Mir Mohamad Sadeghi, *Polym. Compos*., **33**, 843 (2012).
5. P.A.A.P. Marques, T. Trindade, and C.P. Neto, *Compos. Sci. Technol*., **66**, 1038 (2006).
6. Y.Z. Wan, L. Hong, S.R. Jia, Y. Huang, Y. Zhu, Y.L. Wang, and H.J. Jiang, *Compos. Sci. Technol*., **66**, 1825 (2006).
7. D. Ruan, Q. Huang, and L. Zhang, *Macromol. Mater. Eng*., **290**, 1017 (2005).
8. C. Vilela, C.S.R. Freire, P.A.A.P. Marques, T. Trindade, C.P. Netoa, and P. Fardimc, *Carbohydr. Polym*., **7**, 1150 (2010).
9. V.K. Sharma, R.A. Yngard, and Y. Lin, *Adv. Colloid Interface Sci*., **145**, 83 (2009).
10. M. Catauro, M.G. Raucci, F. de Gaetano, and A. Marotta, *J. Mater. Sci.: Mater. Med*., **15**, 831 (2004).
11. J.H. Crabtree, R.J. Burchette, R.A. Siddiqi, I.T. Huen, L.L. Hadnott, and A. Fishman, *Perit. Dial. Int*., **23**, 368 (2003).
12. M. Sládková, B. Vlčková, I. Pavel, K. Šišková, and M. Šloufc, *J. Mol. Struct*., **924**, 567 (2009).
13. O. Choi, K.K. Deng, N.J. Kim, L. Ross Jr., R.Y. Surampalli, and Z.Q. Hu, *Water Res*., **42**, 3066 (2008).
14. C. Baker, A. Pradhan, L. Pakstis, D.J. Pochan, and S.I. Shah, *J. Nanosci. Nanotechno*., **5**, 244 (2005).

 DOI 10.1002/pc

15. G. Rodríguez-Gattorno, D. Díaz, L. Rendón, and G.O. Hernández-Segura, *J. Phys. Chem. B*, **106**, 2482 (2002).
16. X.M. Yang and Y. Lu, *Mater. Lett*., **59**, 2484 (2005).
17. L. Rodríguez-Sánchez, M.C. Blanco, M.A. López-Quintela, *J. Phys. Chem. B*, **104**, 9683 (2000).
18. T. Maneerung, S. Tokura, and R. Rujiravanit, *Carbohydr. Polym*., **72**, 43 (2008).
19. H.S. Baruda, C. Barriosa, T. Regiania, R.F.C. Marquesa, M. Verelstb, J. Dexpert-Ghysb, Y. Messaddeqa, and S.J.L. Ribeiro, *Mater. Sci. Eng. C*, **28**, 515 (2008).
20. M. Montazer, F. Alimohammadi, A. Shamei, and M.K. Rahimi, *Carbohydr. Polym*., **87**, 1706 (2012).
21. S.M. Li, N. Jia, J.F. Zhu, M.G. Ma, F. Xu, B. Wang, and R.C. Sun, *Carbohydr. Polym.* **83**, 422 (2011).
22. A.R. Silva and G. Unali, *Nanotechnology*, **22**, 315605, (2011).
23. Z. Liu, B. Guo, L. Hong, and T.H. Lim, *Electrochem. Commun*., **8**, 83 (2006).
24. F. Bensebaa, F. Zavaliche, P. L'Ecuyer, R.W. Cochrane, and T. Veres, *J. Colloid Interface Sci*., **277**, 104 (2004).
25. A. Pal, S. Shah, and S. Devi, *Mater. Chem. Phys*., **114**, 530 (2009).
26. F. Sun, X. Qiao, F. Tan, W. Wang, and X Qiu, *J. Mater. Sci*., **47**, 7262 (2012).
27. H. Mahmoodian and O. Moradi, *Polym. Compos*., **35**, 495 (2014).
28. S.M. Li, N. Jia, M.G. Ma, Z. Zhang, Q.H. Liu, and R.C. Sun, *Carbohydr. Polym.* **86**, 441 (2011).
29. R. Janardhanan, M. Karuppaiah, and N. Hebalkar, *Polyhedron*, **28**, 2522 (2009).
30. N. Lkhagvajav, I. Yasa, E. Celik, M. Koizhaiganova, and Ö. Sari, *Dig. J. Nanomater. Bios*., **6**, 149 (2011).
31. I. Pastoriza-Santos and L.M. Liz-Marzán, *Nano Lett*., **2**, 903 (2002).
32. P.K. Khanna, N. Singh, D. Kulkarni, S. Deshmukh, S. Charan, and P.V. Adhyapak, *Mater. Lett*., **61**, 3366 (2007).
33. Y. Li, P. Leung, L. Yao, Q.W. Song, and E. Newton, *J. Hosp. Infect*., **62**, 58 (2006).
34. B. Wiley, Y. Sun, B. Mayers, Y. Xia, *Chem. Eur. J*., **11**, 454 (2005).
35. Z.L. Wang, *J. Phys. Chem. B*, **104**, 1153 (2000).
36. D.M. Suflet, G.C. Chitanu, and V.I. Popa, *React. Funct. Polym*., **66**, 1240 (2006).
37. S. Kokot, N. Anh, and T.L. Rintoul, *Appl. Spectrosc*., **51**, 387 (1997).
38. C. Pappas, P.A. Tarantilis, I. Daliani, T. Mavromustakos, and M. Polissiou, *Ultrason. Sonochem*., **9**, 19 (2002).
39. S.M. Li, L.H. Fu, M.G. Ma, J.F. Zhu, R.C. Sun, and F. Xu, *Biomass Bioenergy*, **47**, 516 (2012).
40. H. Yang, R. Yan, H. Chen, D.H. Lee, and C. Zheng, *Fuel*, **86**, 1781 (2007).
41. R. Ball, A.C. McIntosh, and J. Brindley, *Combust. Theory Model*, **8**, 281 (2004).
42. Y.J. Zhu, X.L. Hu, and W.W. Wang, *Nanotechnology*, **17**, 645 (2006).
43. I. Washio, Y. Xiong, Y. Yin, and Y. Xia, *Adv. Mater*., **18**, 1745 (2006).
44. T. Xu, L.Z. Wu, Y. Yu, W.Y. Li, and J.F. Zhi, *Mater. Lett*., **114**, 92 (2014).
45. Z.T. Zhang, B. Zhao, and L.M. Hu, *J. Solid State Chem*., **121**, 105 (1996).
46. R. He, X.F. Qian, J. Yin, and Z.K. Zhu, *J. Mater. Chem*., **12**, 3783 (2002).
47. J.S. Kim, E. Kuk, K.N. Yu, J.-H. Kim, S.J. Park, H.J. Lee, S.H. Kim, Y.K. Park, Y.H. Park, C.-Y. Hwang, Y.-K. Kim, Y.-S. Lee, D.H. Jeong, and M.-H. Cho, *Nanomed-nano Technol*., **3**, 95 (2007).
48. V.K. Sharma, R.A. Yngard, and Y. Lin, *Adv. Colloid Interface Sci*., **145**, 83 (2009).
49. A. Henglein, *J. Phys. Chem*., **97**, 5457 (1993).
50. C.N. Lok, C.M. Ho, R. Chen, Q.Y. He, W.Y. Yu, H.Z. Sun, P.K.H. Tam, J.F. Chiu, and C.M. Che, *J. Biol. Inorg. Chem*., **12**, 527 (2007).
51. A. Henglein, *Chem. Mater*., **10**, 444 (1998) .